J. Fluid Mech. (1988), *vol.* 193, *pp.* 111–127
Printed in Great Britain

Low-Reynolds-number instabilities in stagnating jet flows

By J. O. CRUICKSHANK
Avco Research Laboratory Textron, 2385 Revere Beach Parkway, Everett, MA 02149, USA

(Received 14 August 1987 and in revised form 2 December 1987)

A theoretical model is developed for predicting the critical plate–orifice distances for viscous fluid buckling in plane and axisymmetric low-Reynolds-number bounded jets in stagnation flow. The theory is based on a hypothesis that treats the spatial growth of perturbation to the jet in a manner that distinguishes between the near-wall and far-field regions of the jet. This perturbation growth rate is shown to be the important parameter in the determination of the critical plate–orifice distances.

This study also uses a one-dimensional model of the fluid column when it is displaced from equilibrium to determine the frequency at which buckling is first initiated in the case of the plane jet.

1. Introduction

The low-Reynolds-number instability observed when a high-viscosity fluid jet flows vertically against a flat surface, and commonly referred to as fluid buckling, has been the subject of several studies in recent years. Taylor (1968) first brought this phenomenon to the attention of the scientific community. Experimental work aimed at quantifying this behaviour in terms of the common fluid mechanical parameters was subsequently reported by Cruickshank (1980) and Cruickshank & Munson (1981).

The term fluid buckling has since been extended by Bejan to a large class of meandering flows of which viscous fluid buckling is but a subset. A summary of the current state of the subject is given in his review article (Bejan 1987) where an exhaustive bibliography is also provided.

Figures 1 and 2 show an axisymmetric jet and a plane jet respectively undergoing the low-Reynolds-number instability we call viscous fluid buckling. Detailed descriptions of the observed behaviour during and subsequent to the onset of the instability are provided in Cruickshank (1980) and Cruickshank & Munson (1981). In the developments that follow, theoretical models will be developed for predicting the critical height at which the instabilities first appear in plane and axisymmetric jets. Qualitative explanations will also be provided for some of the peculiar features of viscous fluid buckling that were documented by these workers. Cruickshank & Munson (1983) have provided a model for the buckling frequency at different plate–orifice distances for the case of the round jet. This paper now provides a model for the frequency at the onset of buckling for the case of the plane jet.

2. The mechanics of fluid buckling: a hypothesis

In the following development, we assume that the problem of fluid buckling can be analysed by considering the stagnation jet flow as consisting of two distinct

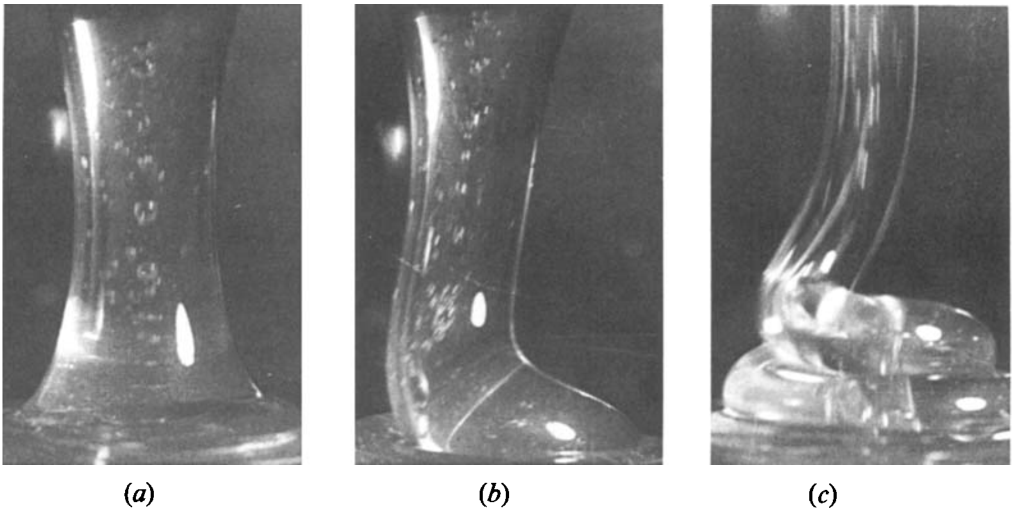

FIGURE 1. The buckling of a fluid column. (a) Axisymmetric jet in stagnation flow. (b) Axisymmetric jet at point of buckling. (c) The coiling that exists after buckling.

regions: the far-field region in which the jet diameter is assumed constant, and a near-wall region where the wall's effects are concentrated. Disturbances of the far-field jet are assumed to grow exponentially in the flow direction with a growth rate parameter designated α, and in the near-wall region to decay at a decay rate consistent with the requirement that the no-slip condition be met at the wall. These two growth and decay parameters, in spite of having these distinct behavioural characteristics in their respective regions, are expected to have equal values (for continuous transition from the far-field to the near-wall) at the line separating these two regions.

For an axisymmetric jet flowing against a flat surface the no-slip condition suggests that the near-wall value of α should be such that the perturbation velocities decay in the wall region. Hence α should be (in a local sense) of the form

$$\alpha = k\frac{H'}{d^2},$$

at or near the wall. The coefficient k is a proportionality constant which we will arbitrarily set equal to 1.0, d is the local jet diameter and H' is the distance from the orifice to some point in the wall region. Hence $\alpha \rightarrow 0$ as H' and $d \rightarrow \infty$ and the perturbation velocities will decay accordingly for all values of H'.

If the plate–orifice distance is H, and the thickness of the wall region is Δz, then from figure 3, the transition line is at a distance $H - \Delta z$ from the orifice. The maximum near-wall value of α thus occurs at the transition line with a value equal to $(H - \Delta z)/d_0^2$ since d increases rapidly in this region. d_0 is the constant diameter of the far-field portion of the jet.

Physical observation indicates that the transition line tends to move closer to the plate as the plate–orifice distance increases and thus the deceleration rate in the wall region is expected to increase significantly as the thickness of the wall region decreases. Indeed, in the limit $\Delta z \rightarrow 0$, the deceleration rate could become infinite,

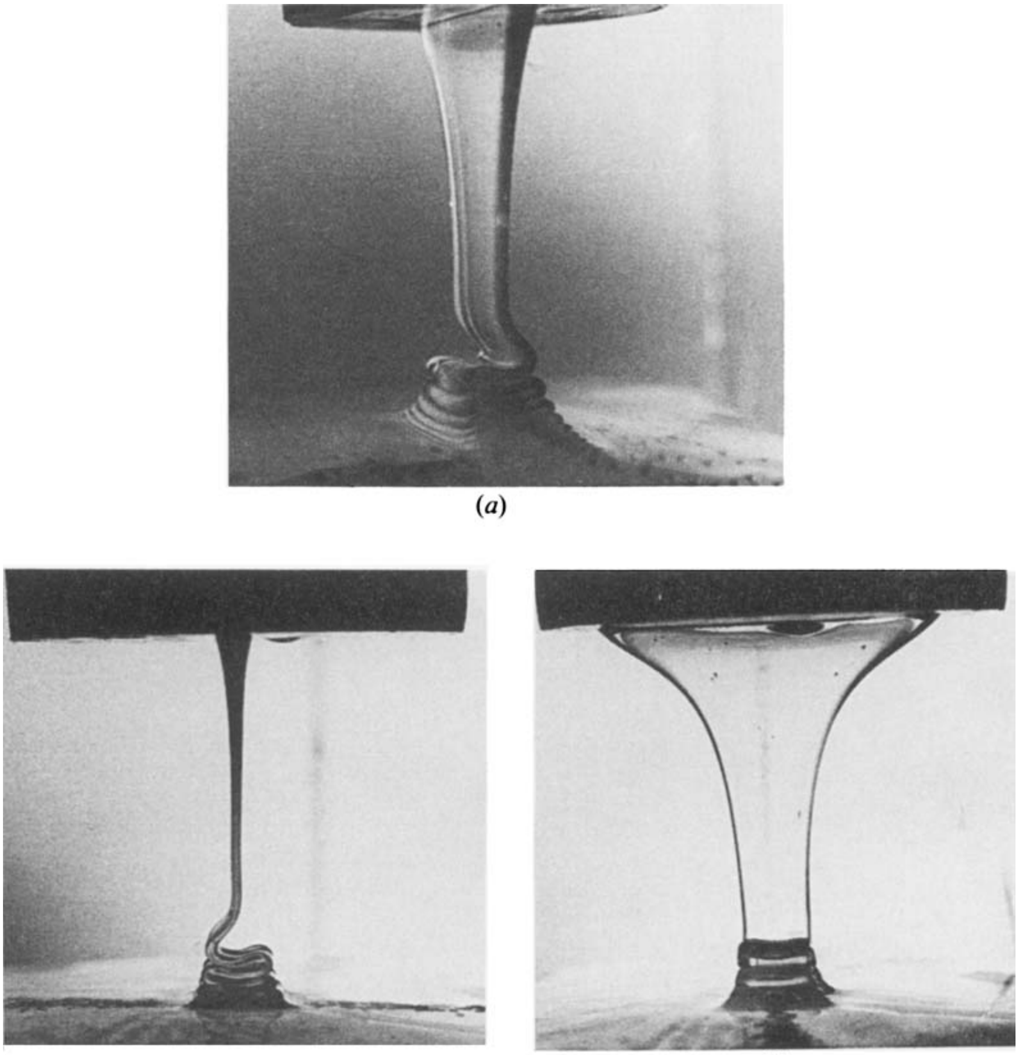

(*a*)

(*b*) (*c*)

FIGURE 2. Folding of a plane unstable jet. (*a*) A three-dimensional view. (*b*) Side view. (*c*) Front view ($D \times d_1 = 0.414$ cm $\times$ 4.14 cm).

clearly, a physically implausible condition which can only be negated if the transition from the far-field to the near-wall region became a discontinuous one. This critical condition when this discontinuity first appears corresponds to a near-wall value of α equal to H/d_0^2.

Figure 3 shows an expanded view of the region near the wall. The jet diameter near the wall is assumed to go smoothly to infinity and the thickness of this region is assumed to be very small. In figure 3, 0–*a*, 0–*b* and 0–*c* represent the possible relative magnitudes of the far-field perturbation velocities when they are less than, equal to, or greater than their corresponding maximum possible value in the wall region, also given by 0–*b*. Note that the thickness of the wall region is considered negligible ($\Delta z \rightarrow 0$) in cases 0–*b* and 0–*c*.

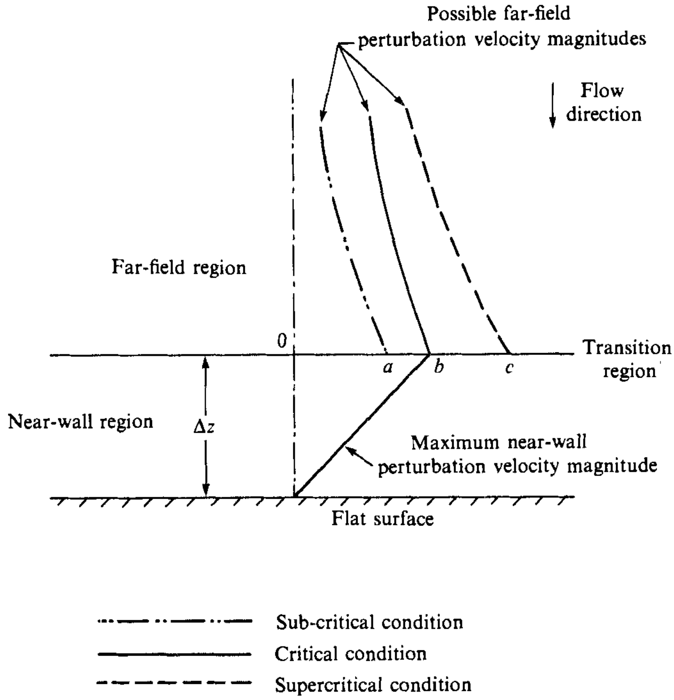

FIGURE 3. The transition region near a flat surface.

Case 0–b is synonymous with the critical condition described above and 0–c indicates that the no-slip condition cannot be met at the wall without the fluid undergoing the discontinuous transition alluded to earlier.

A discontinuity at this transition line would imply discontinuities in the local shear stresses between the two regions. For a perfectly vertical jet flowing against a perfectly flat surface, this may be of no consequence to the flow. In the absence of these perfect conditions, a net shear force could arise at the transition line effectively pulling the jet column in the direction of this net force and away from the jet centreline.

The initial stages of viscous fluid buckling would then have been initiated. Large compressive stresses would arise at the interface due to the decelerations inherent in the discontinuity. The fluid column according to this hypothesis, would have started sliding away from its equilibrium position. This displacement from equilibrium leads to the initiation of an oscillatory motion of fixed frequency, the mechanics of which will be demonstrated in §5. The ensuing frequency will be calculated in the case of a plane jet, in §6.

Thus we propose that the critical condition for the onset of buckling of a jet in the absence of gravitational or surface tension forces is that the transition line occurs at or very close to the plate surface and hence from the near-wall condition,

$$\alpha_{\text{critical}} = H/d^2.$$

Since the far-field value of the perturbation growth rate, α must always equal the near-wall value at the transition line, this implies that fluid buckling will occur when

$$\frac{H_c}{d^2} = \alpha_{\text{far-field}},$$

where d is the jet diameter, d_0, for a round jet or the jet thickness, d_1, for a plane jet. H_c is the critical plate–orifice distance.

In the following sections, we will determine the far-field values of α for the two cases of round and plane jets so as to predict the critical plate–orifice distances for buckling for these jet geometries based on the hypothesis of this section.

3. The governing equations for azimuthal instability in round jets

We now consider the problem of azimuthal instability in low-Reynolds-number bounded round jets. We adopt an approach based on that of Batchelor & Gill (1962) with appropriate modifications for this specific problem.

The perturbation velocity is $\boldsymbol{u}$ with components u_x, u_r and u_ϕ in cylindrical (x, r, ϕ) coordinates. If the main jet has constant axial velocity U, then the momentum equation is

$$\frac{\partial \boldsymbol{u}}{\partial t}+U\frac{\partial \boldsymbol{u}}{\partial x} = -\frac{1}{\rho}\boldsymbol{\nabla} p+\nu\nabla^2\boldsymbol{u}, \tag{1}$$

where p is the perturbation pressure, ρ is the fluid density and ν is the kinematic viscosity. Conservation of mass results in the continuity equation

$$\boldsymbol{\nabla}\cdot\boldsymbol{u} = \frac{\partial u_x}{\partial x}+\frac{1}{r}\frac{\partial}{\partial r}(ru_r)+\frac{1}{r}\frac{\partial u_\phi}{\partial \phi} = 0. \tag{2}$$

We assume these velocity components to be of the form

$$u_x, u_r, u_\phi = R\,[\{F(r), G(r), \mathrm{i}H(r)\}\,\mathrm{e}^{\mathrm{i}n\phi+\alpha x-\alpha ct}], \tag{3}$$

and the perturbation pressure is

$$\frac{p}{\rho} = R\,[P(r)\,\mathrm{e}^{\mathrm{i}n\phi+\alpha x-\alpha ct}]. \tag{4}$$

The substition of (3) and (4) into (1) and (2) produces the following:

$$-\alpha cF+\alpha UF = -\alpha P+\nu\left\{F'+\frac{1}{r}F''-\left(\frac{n^2}{r^2}-\alpha^2\right)F\right\}, \tag{5}$$

$$-\alpha cG+\alpha UG = -P'+\nu\left\{G''+\frac{1}{r}G'-\left(-\alpha^2+\frac{n^2+1}{r^2}\right)G+\frac{2n}{r^2}H\right\}, \tag{6}$$

$$-\alpha cH+\alpha UH = -\frac{nP}{r}+\nu\left\{H''+\frac{1}{r}H'-\left(-\alpha^2+\frac{n^2+1}{r^2}\right)H+\frac{2n}{r^2}G\right\}, \tag{7}$$

$$\alpha F+G'+\frac{1}{r}G-n\frac{H}{r} = 0. \tag{8}$$

For the case $n = 1$, (5) may be rewritten as follows:

$$F''+\frac{1}{r}F'-\left(\frac{1}{r^2}-m^2\right)F = \frac{\alpha P}{\nu}, \tag{9}$$

where
$$m^2 = \alpha^2-\frac{U\alpha}{\nu}+\frac{c\alpha}{\nu},$$

or
$$m^2 = \alpha^2-\frac{U^*\alpha}{\nu} \quad \text{if} \quad U^* = (U-c). \tag{10}$$

We assume a pressure variation given by

$$P(r) = BJ_1(\beta r). \tag{11}$$

Then (9) is satisfied by

$$F(r) = AJ_1(mr) + \frac{\alpha B}{\nu(m^2-\beta^2)} J_1(\beta r). \tag{12}$$

The physical requirement that $F(r)$ be bounded at $r = 0$ is satisfied by (12).

We also choose a solution to (7) so that

$$G(r) = \frac{Br}{2\nu} J_1(\beta r) + H(r), \tag{13}$$

then

$$H'' + \frac{1}{r}H' + m^2 H = 0, \tag{14}$$

and here also, the physical condition of boundedness on $H(r)$ implies that

$$H(r) = EJ_0(mr). \tag{15}$$

In order to satisfy mass conservation requirements, (8) must govern the relationship between $F(r)$, $G(r)$ and $H(r)$. Hence from continuity:

$$(\alpha A - Em) J_1(mr) + B\left[\frac{\beta r}{2\nu} J_0(\beta r) + \frac{1}{2\nu} J_1(\beta r) + \frac{\alpha^2}{\nu(m^2-\beta^2)} J_1(\beta r)\right] = 0. \tag{16}$$

This is satisfied if $\alpha A = Em$ and $B = 0$.

There must be continuity of the normal stress across the jet boundary and therefore, if p_a is the pressure in the inviscid, stationary outer medium, and p_b the pressure in the jet, then at the interface between the two fluids

$$-p_a = -p_b + 2\mu \left.\frac{\partial u_r}{\partial r}\right|_{r=a},$$

or in non-dimensional terms

$$-p_a = -p_b + 2\left.\frac{\partial u_r/\partial r}{Re}\right|_{r=a},$$

where Re is the Reynolds number.

If we neglect the density of the quiescent outer medium, then $p_a = 0$ and the boundary condition becomes

$$0 = -p_b + 2\left.\frac{\partial u_r/\partial r}{Re}\right|_{r=a}.$$

For low-Reynolds-number flows of the type under discussion here, it is necessary for $(\partial u_r/\partial r)|_{r=a}$ to be zero to ensure that the perturbation pressure at the interface p_b does not itself acquire unreasonably large values which would be inconsistent with its being a perturbation quantity. Hence we may write

$$p_b = 0,$$

and

$$\left.\frac{\partial u_r}{\partial r}\right|_{r=a} = 0. \tag{17}$$

Substituting for u_r in (17), we have

$$mJ_1(ma) = 0, \tag{18}$$

hence

$$\left.\begin{aligned} J_1(ma) &= 0, \\ ma &= 3.8317, \ldots \end{aligned}\right\} \tag{19}$$

and

A consequence of (10) is that

$$\alpha = \frac{U^*}{2\nu} + \frac{1}{2}\left[\frac{U^{*2}}{\nu^2} + 4m^2\right]^{\frac{1}{2}} \tag{20}$$

where m is given by (19), and hence the critical plate–orifice distance, from the hypothesis of §2 is given by

$$\frac{H_c}{d_0} = \tfrac{1}{2}Re + \tfrac{1}{2}[Re^2 + 234.9]^{\frac{1}{2}}, \tag{21}$$

for the case of azimuthal instability where

$$Re = \frac{U^* d_0}{\nu},$$

or for the small Reynolds numbers involved,

$$\frac{H_c}{d_0} = 7.6634. \tag{22}$$

For the case studied in this section, the existence of a tangential stress component suggests that the motion that would accompany the discontinuity will be of a rotatory nature.

It can easily be shown, using techniques similar to those in the development above, that for a non-azimuthal ($n = 0$) two-dimensional treatment of the round jet, the corresponding value of α is $4.8096/d_0$, hence based on the earlier hypothesis, the critical buckling height of a round jet for a purely two-dimensional, and hence a pendulum-like, oscillation is given by $H_c/d_0 = 4.8096$. This mode of buckling is known to occur (Cruickshank & Munson 1981) but is not the preferred mode. The helical or rotatory mode ($n = 1$) treated earlier, appears to be the preferred mode.

We continue this analysis by studying the conditions under which a plane jet in stagnation flow would behave according to the scenario of §2.

4. Instability in a plane jet

Consider a plane two-dimensional jet flowing with constant velocity U in the axial direction, x. The equations obtained from a perturbation analysis of the jet column for perturbation velocities u, v are the continuity equation

$$\frac{\partial u}{\partial x} + \frac{\partial v}{\partial y} = 0, \tag{23}$$

and the two momentum equations:

$$\frac{\partial u}{\partial t} + U\frac{\partial u}{\partial x} = -\frac{1}{\rho}\frac{\partial p}{\partial x} + \nu\left(\frac{\partial^2 u}{\partial x^2} + \frac{\partial^2 u}{\partial y^2}\right), \tag{24}$$

$$\frac{\partial v}{\partial t} + U\frac{\partial v}{\partial x} = -\frac{1}{\rho}\frac{\partial p}{\partial y} + \nu\left(\frac{\partial^2 v}{\partial x^2} + \frac{\partial^2 v}{\partial y^2}\right). \tag{25}$$

Let
$$v = -\frac{\partial \Psi}{\partial x}, \quad u = \frac{\partial \Psi}{\partial y},$$

then if we eliminate pressure between the two momentum equations, we obtain

$$\left(-\frac{\partial}{\partial t}+\nu D-U\frac{\partial}{\partial x}\right)D\Psi = 0,$$

where
$$D = \frac{\partial^2}{\partial x^2}+\frac{\partial^2}{\partial y^2},$$

and Ψ is the perturbation streamfunction. Let the streamfunction's dependence on the axial distance x be proportional to $e^{\alpha x}$, and on time to $e^{-\alpha ct}$ then if

$$m^2 = \alpha^2-\frac{U^*\alpha}{\nu}, \tag{26}$$

we have
$$\left(\frac{d^2}{dy^2}+m^2\right)\left(\frac{d^2}{dy^2}+\alpha^2\right)\Psi(y) = 0. \tag{27}$$

We define $\chi_1(y)$ and $\chi_2(y)$ such that (Basset 1894)

$$\Psi = \chi_1+\chi_2,$$

then
$$\frac{d^2\chi_1}{dy^2}+m^2\chi_1 = 0, \tag{28}$$

and
$$\frac{d^2\chi_2}{dy^2}+\alpha^2\chi_2 = 0. \tag{29}$$

Hence
$$\Psi(y) = A\sin my+B\cos my+C\sin\alpha y+D\cos\alpha y. \tag{30}$$

Since $d\Psi/dy$ must be an even function, $B = D = 0$.

The pressure is obtained from (25) which is equivalent to

$$\frac{\partial p}{\partial y} = \rho U^*\alpha^2\chi_2, \tag{31}$$

and
$$p(y) = -\rho U^* C\alpha\cos\alpha y+\text{constant}, \tag{32}$$

where the exponential factor has been omitted for brevity.

Similar considerations for the outside, stagnant medium with negligible density gives $p(y) = $ constant, and setting this constant to zero results in the following condition at the jet interface

$$-C\alpha\cos\alpha\tfrac{1}{2}t = 0, \tag{33}$$

where t is the jet thickness.

From (33)
$$\cos\tfrac{1}{2}\alpha t = 0, \tag{34}$$

hence
$$\tfrac{1}{2}\alpha t = \tfrac{1}{2}\pi, \tfrac{3}{2}\pi, \ldots \tag{35}$$

or in terms of jet thickness d_1

$$\alpha d_1 = (2n+1)\pi \quad (n = 0, 1, \ldots), \tag{36}$$

and the critical non-dimensional plate–orifice distance for buckling in a plane jet is, according to our hypothesis, given by

$$H_c/d_1 = (2n+1)\pi \quad (n = 0, 1, \dots). \tag{37}$$

In the next section, a simple one-dimensional model of the jet after displacement from equilibrium (from the hypothesis of §2, is developed and used for obtaining the frequency of the oscillations that are observed after this displacement occurs for the case of a plane jet.

5. The consequences of a displacement of the jet column

Cruickshank (1980) has shown that the linearized equation governing the transverse motion of a thin fluid column is of the following form which, for small displacements, is exact for thin, shear-free flows

$$(T-mv^2)\frac{\partial^2 y}{\partial x^2} - 2mv\frac{\partial^2 y}{\partial x\,\partial t} - m\frac{\partial^2 y}{\partial t^2} - mg\frac{\partial y}{\partial x} = 0, \tag{38}$$

where T = axial tensile force, m = mass/unit length of the fluid, v = axial velocity along the jet = U, g = acceleration due to gravity, y = displacement of jet from equilibrium, x = axial distance along the jet. A complete derivation of the two-dimensional equivalent of (38) is also to be found in Cruickshank (1987).

The assumption that T, m and v are not functions of y has its basis in the classical linearized modelling of vibrating media. Ideally, the tension in a vibrating string, for example, must change with vertical position. Linear models do not include this effect. Another example of this was the study of the moving vibrating threadline where the velocity was assumed constant (Swope & Ames 1963), although clearly this is not the case since it has to have a vertical time-dependent component. We use these same assumptions in this model.

Consider the oscillation equation with spatially constant T, m, and v. When the stagnating fluid jet is slightly displaced from its equilibrium position, for the reasons stated in §2, we expect that this change in geometry will result in very small time-dependent changes in the value of the normal compressive force set up by the discontinuity in the perturbation velocities.

To model this time dependency, we assume that

$$T = -T_0 + \phi(t), \tag{39}$$

where $-T_0$ represents the initial constant compressive force within the fluid caused by the discontinuity and $\phi(t)$ is a very small perturbation on this value. Expanding $\phi(t)$ in a Fourier series and retaining only the first terms gives

$$T = -T_0 + T_t \cos\theta t. \tag{40}$$

Then substituting for T in the oscillation equation, we have

$$(-T_0 + T_t\cos\theta t - mv^2)\frac{\partial^2 y}{\partial x^2} - 2mv\frac{\partial^2 y}{\partial x\partial t} - m\frac{\partial^2 y}{\partial t^2} - mg\frac{\partial y}{\partial x} = 0. \tag{41}$$

For the fluid-buckling problem, photographs (figure 1 for example) indicate that $y(x,t) \cong e^{\lambda x} y_1(t)$ is a reasonable approximation of the displaced motion. Here λ is assumed constant. Note that v is still presumed to be a constant for the purpose of this model.

Based on Bolotin's (1964) approach to a similar problem, we let $y_1(t) = U(t)\,c(t)$, where $c(t) = C\mathrm{e}^{-v\lambda t}$ and c is a constant. Thus, we obtain

$$\ddot{U}+\Omega_\lambda^2\left(1+\frac{mg}{\lambda T_0}-2\mu^*\cos\theta t\right)U = 0, \tag{42}$$

where
$$\Omega_\lambda^2 = \frac{T_0\lambda^2}{m}, \quad (\dot{\ }) = \frac{\mathrm{d}}{\mathrm{d}t}, \tag{43a}$$

and
$$2\mu^* = \frac{T_t}{T_0}. \tag{43b}$$

From (42) we may infer that the impact on the fluid column of the initial displacement from equilibrium combined with the compressive load arising from the discontinuity, may be the imposition of a transient physical motion whose characteristics are determined by (42) and (43a, b).

According to the Mathieu equation stability diagram (Bolotin 1964) the first critical point for instability corresponds to the value of θ such that

$$\frac{\theta}{2\Omega_\lambda} = 1.0.$$

In the real world where disturbances are random, θ is essentially arbitrary, hence this condition is not a difficult one to meet. For the specific model under consideration here (negligible surface tension and gravitational forces with constant jet diameter in the region away from the wall) the requisite compressive stress arises only when the discontinuity in the perturbation velocities occurs. In the absence of that effect, the stress along the jet is either zero (constant diameter jet) or positive (if there is acceleration under gravity). For either of these conditions, Ω_λ is either zero or it has no real value. Thus no self-sustaining oscillations can take place and the jet is stable. Hence these self-sustaining oscillations take place only because of the existence of the compressive stress set up by the discontinuities in the perturbation velocities.

Mathieu's equation (42) indicates that the self-sustaining oscillation occurs at a frequency given by

$$\Omega_{\lambda,g} = \Omega_\lambda\left(1+\frac{mg}{\lambda T_0}\right)^{\frac{1}{2}}, \tag{44}$$

and (44) suggests that these oscillations can take place in the absence of gravity; that is, with $g = 0$. Cruickshank & Munson (1981) have shown photographs of such oscillations in the horizontal plane.

6. Predicting the critical buckling frequency for a plane jet

From (44), the critical frequency at which fluid buckling is first initiated is given, in the absence of gravitational effects, by (43a):

$$\omega^2 = \frac{T_0}{m}\lambda^2.$$

The model used here, with proper interpretation of the T and m terms, would be applicable to both axisymmetric and plane jets. Comparisons of the earlier perturbation model and the model of §5 suggests that α and λ may be the same, thus it appears possible to predict the frequency that accompanies buckling.

From (37) it is not clear which value of n would correspond to the experimentally observed condition, however, the data (with which comparisons will be shown shortly) appear to indicate that the case $n = 1$ is the preferred mode.

Consider the case of the plane jet. From (36), using $n = 1$, we have

$$\alpha d_1 = 3\pi,$$

hence

$$\left.\begin{aligned} \alpha = \lambda &= \frac{3\pi}{d_1}, \\ \omega^2 &= \frac{T_0}{m}\left(\frac{3\pi}{d_1}\right)^2. \end{aligned}\right\} \tag{45}$$

or

Cruickshank & Munson (1982) have shown that the compressive stress σ_0 associated with fluid buckling is of the form

$$\frac{2\sigma_0}{\rho v_1^2} = 4\alpha^* (1-\alpha^*)/(1+\alpha^*)^2. \tag{46}$$

In (46), ρ is the fluid density, v_1 is the fluid velocity in the main jet and α^* is an energy loss coefficient associated with fluid buckling.

α^* has a value given by $0.65 \leqslant \alpha^* \leqslant 0.75$ for the plane jet, with a reported average value of 0.70. For the axisymmetric jet the average value of α^* is 0.76.

For the plane jet, if we use the average value of α^* in (46), an estimate of the compressive stress at buckling is thus given by

$$\frac{\sigma_0}{\rho v_1^2} = 0.145. \tag{47}$$

Using (45) and (47) we can show for the plane jet that

$$\omega(d_1/g)^{\frac{1}{2}} = 3.585\left(\frac{\mu Q'}{\gamma d_1^3}\right)\left(\frac{g d_1^3}{\nu^2}\right)^{\frac{1}{2}}, \tag{48}$$

at the onset of buckling, where d_1 is the thickness of the jet and Q' is the volume flow rate per unit slit width. In (48), the gravity term has been added to both sides of the equation in order to generate non-dimensional terms that are consistent with those that were used in the presentation of the experimental data.

The model developed here would be applicable to a plane jet of infinite width since the additional effects that would arise in jets of finite width D were ignored. Indeed, dimensional analysis (Cruickshank 1980) shows that there is likely to be a dependence on the non-dimensional parameter D/d_1 if the flow is not purely one-dimensional. Figure 2 clearly indicates that these added effects cannot be ignored if we are to model the experimental conditions reasonably accurately.

The choice of a correction factor must be determined by the observed fact that the oscillation frequency of the jet scales with the inverse of the D/d_1 ratio. Secondly, the width of the jet at the buckling location is smaller than that near the slit (figure 2). Thus the mean flow rate per unit width is in reality higher at the buckling point than it is when based on the slit width. Figure 2 suggests that the ratio between the two values may be approximately equal to 4 for the case $D/d_1 = 10.0$.

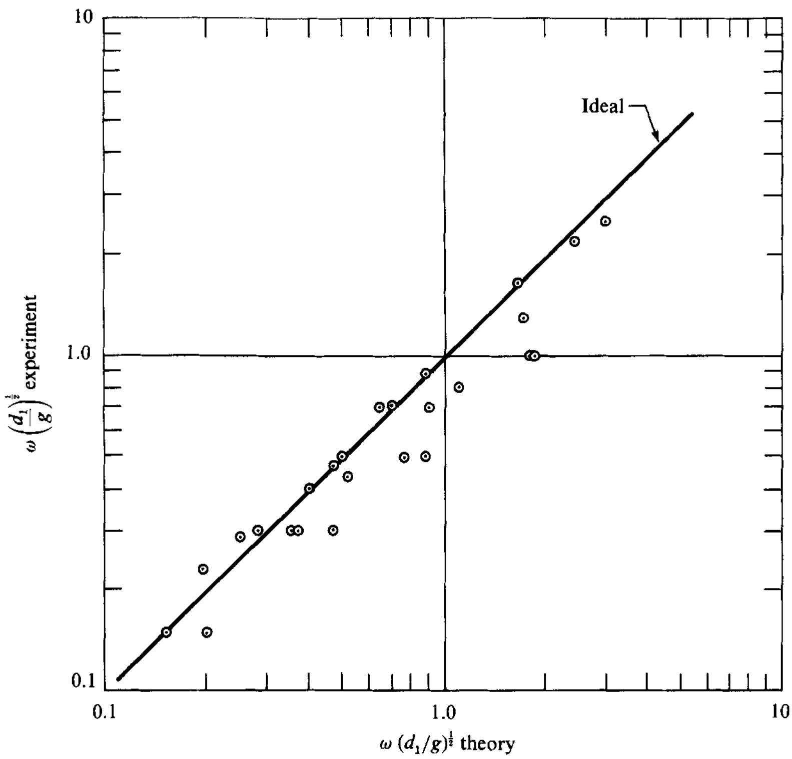

FIGURE 4. Theory *vs.* experiment: Frequency at onset of buckling for plane jet. $D \times d_1 = 10.0$.

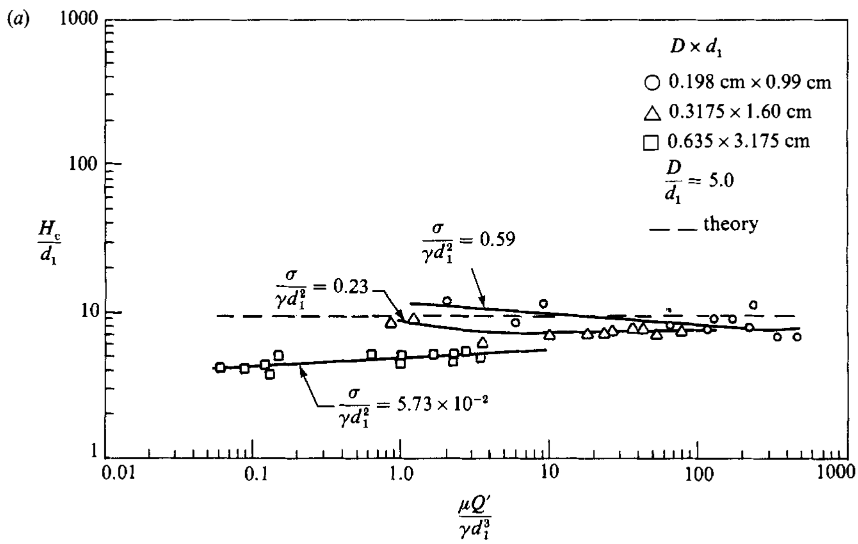

FIGURE 5(*a*). For caption see facing page.

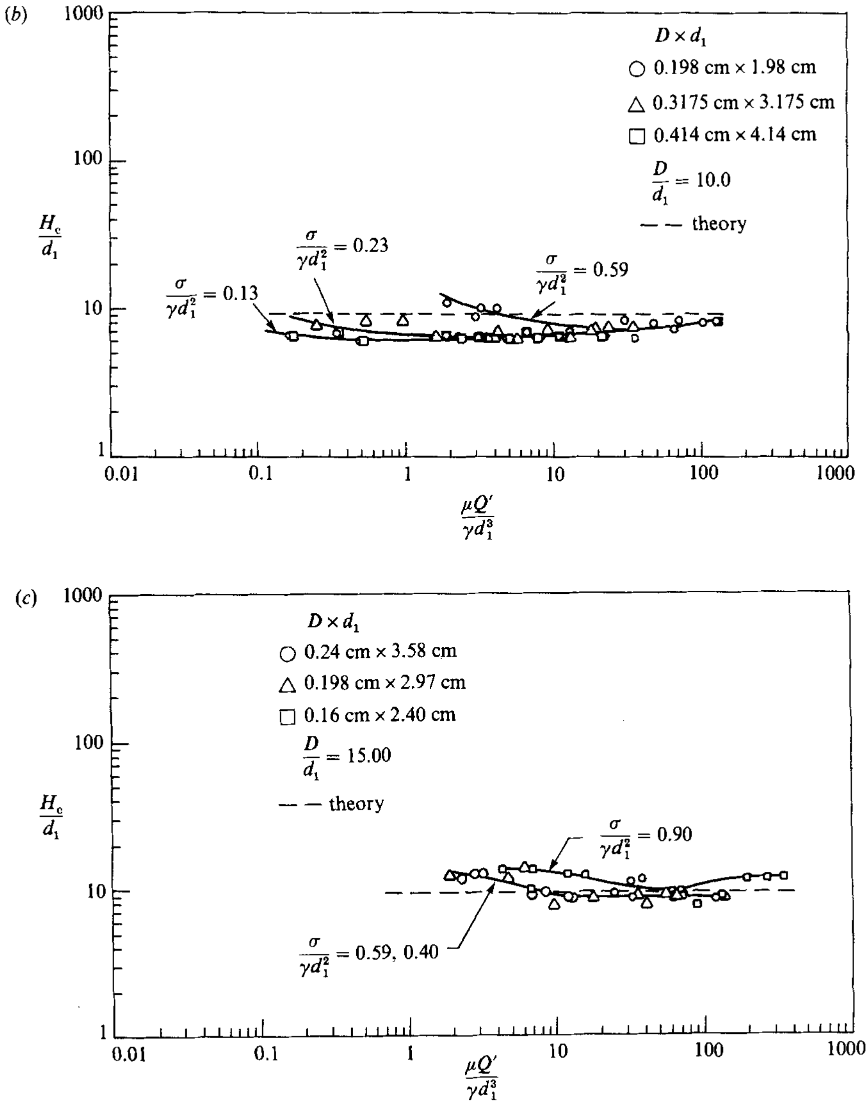

FIGURE 5. Comparisons of theoretical prediction and experimental data: critical buckling height for plane jet.

We therefore use a correction factor for these geometrical effects and for surface tension effects, of the form

$$C = \frac{2}{3}\left[4\left(\frac{D}{d_1}\right)^{-1} - \left(\frac{\sigma}{\gamma d_1^2}\right)^3\right]. \tag{49}$$

The non-dimensional frequency at the onset of buckling then becomes (for $D/d_1 = 10.0$)

$$\omega\left(\frac{d_1}{g}\right)^{\frac{1}{2}} = 2.39\left(\frac{\mu Q'}{\gamma d_1^3}\right)\left(\frac{g d_1^3}{\nu^2}\right)^{\frac{1}{2}}\left[4\left(\frac{D}{d_1}\right)^{-1} - \left(\frac{\sigma}{\gamma d_1^2}\right)^3\right]. \tag{50}$$

Figure 4 shows a comparison of the measured non-dimensional frequency (Cruickshank 1980) versus that predicted by (50). The comparison is relatively good.

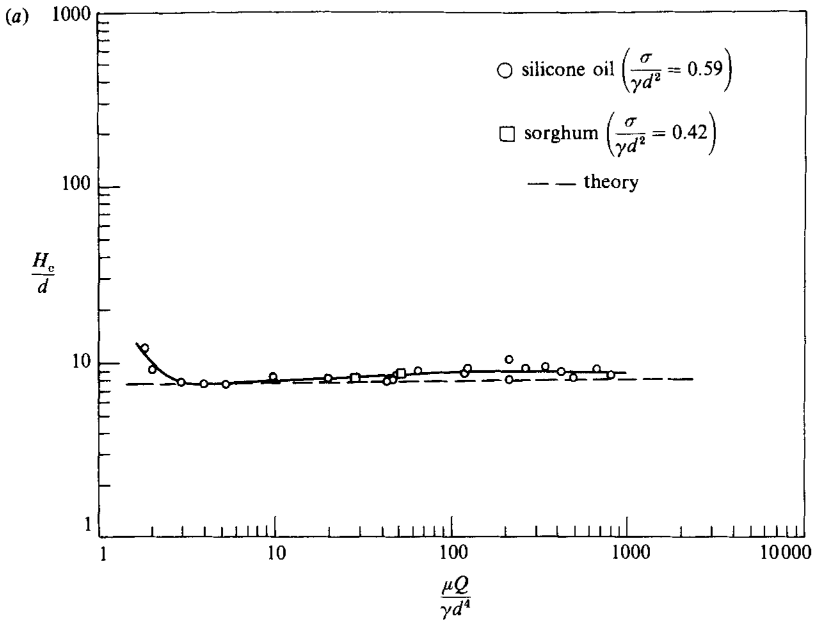

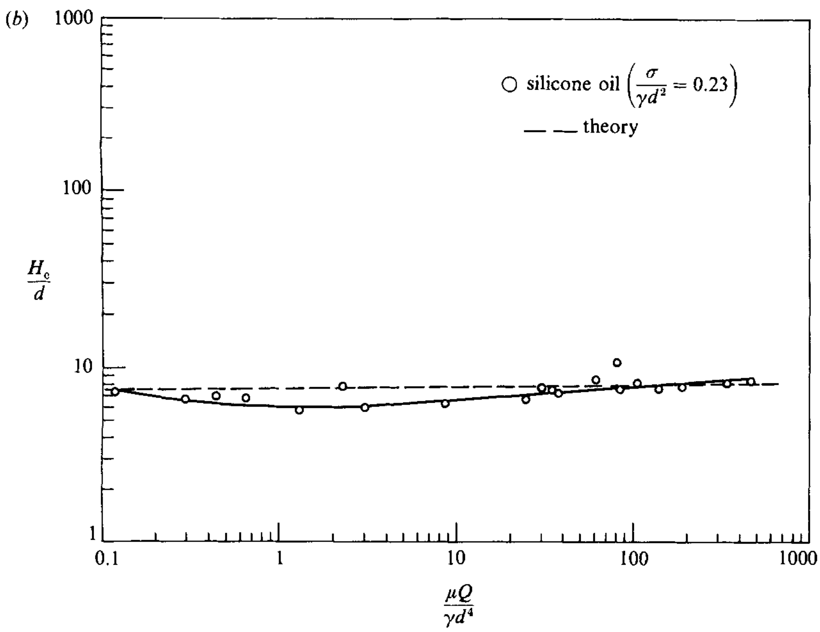

FIGURE 6(a, b). For caption see facing page.

There is a fair amount of scatter in the measured values of the energy loss coefficient used here (Cruickshank & Munson 1982) and so the fact that there is some scatter here is not too surprising.

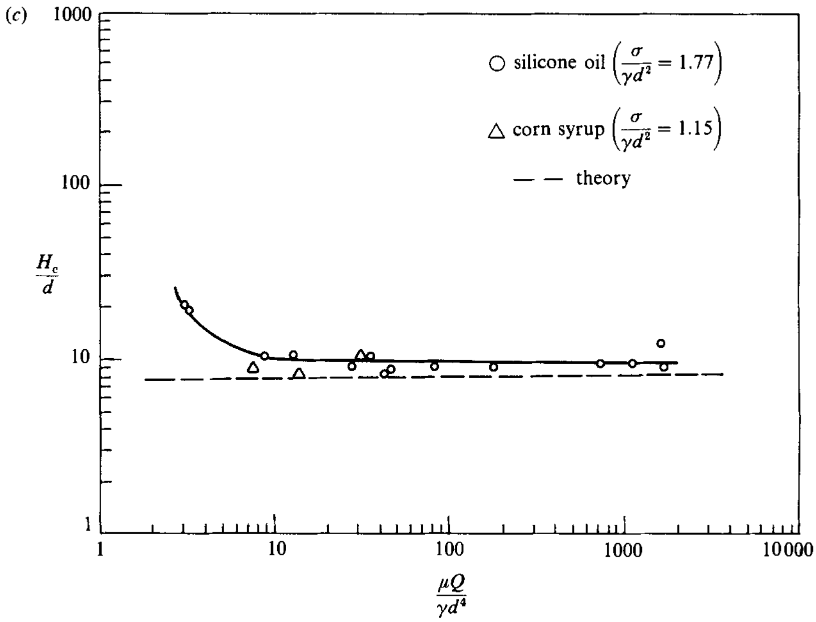

FIGURE 6. Comparisons of theoretical prediction and experimental data: critical buckling height for axisymmetric jet.

7. Results and discussions

Figures 5(*a–c*) and 6(*a–c*) show comparisons with experimental data (Cruickshank 1980) of the predicted critical non-dimensional plate-orifice distance at which buckling is first initiated, for the plane jet and the axisymmetric jet respectively.

From figures 5(*a–c*) and 6(*a–c*), it is clear that there is very good agreement with the experimental data at relatively high values of the flow rate parameter (> 10.0). At relatively low flow rates, there is divergence between the theory and the experimental data that appears to be a surface tension effect. This is not unexpected. At low enough flow rates, surface tension effects are expected to dominate, leading to the break up of the jet. Hence it is not surprising that the effect of surface tension begins to make itself felt more and more as the flow rate goes down.

The buckling height for the plane jet appears to correspond to the case $n = 1$, which is 3π. For the axisymmetric jet, the azimuthal value ($n = 1$) also appears to be the dominant buckling mode (Cruickshank 1980) and these values were used in the comparisons. Figure 7, which consists of critical plate-orifice distances for axisymmetric jets with very small values of

$$g\frac{d_1^3}{\nu^2}, \quad \frac{\sigma}{\gamma d_1^2},$$

tends to indicate, however, that the non-azimuthal mode may be the dominant form for axisymmetric jets when gravitational, surface tension and flow rate effects are all very small.

In the absence of gravitational effects, small values of the surface tension and flow rate parameters would appear to be the necessary pre-requisite for an initial non-azimuthal buckling mode. Thus large diameter jets would be more prone to this type of buckling than small diameter ones, as confirmed by Cruickshank & Munson (1981).

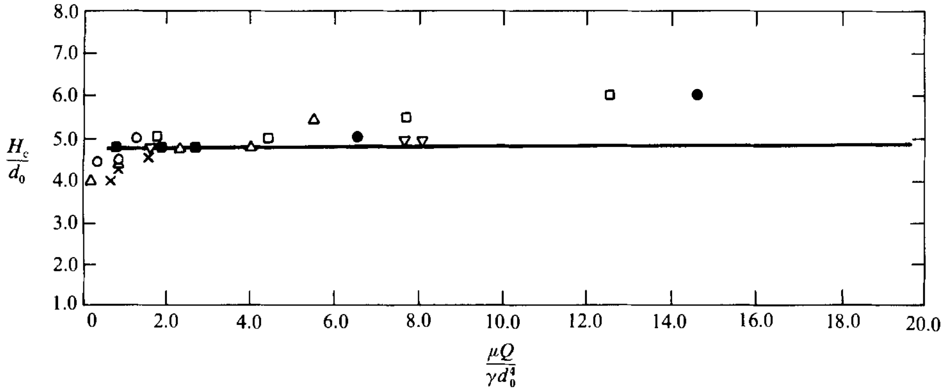

FIGURE 7. Critical buckling heights for axisymmetric jets with low surface tension and flow rate parameters. Values of gd^3/ν^2: ■, 2.23×10^{-2}; ○, 3.33×10^{-4}; △, 8.49×10^{-2}; □, 2.57×10^{-2}; ●, 2.85×10^{-3}; ×, 8.48×10^{-2}; ▽, 9.42×10^{-3},——, theory.

In the presence of gravity, the jet diameter narrows as the plate is moved further away from the orifice and a transition to the azimuthal mode would be expected to occur at some point. From the experimental data (Cruickshank & Munson 1981), it appears that this occurs in a chaotic transition region in which both the azimuthal and non-azimuthal modes appear intermittently, producing a random behaviour that was difficult to characterize experimentally.

The results of the perturbation analysis of the earlier sections indicate that when the axisymmetric jet becomes initially unstable in the pendulum mode, the helical instability may kick in at its critical value of H/d. Based on the theory developed in those sections, the ratio of plate–orifice distances between the onset of the pendulum mode and its transition to the helical mode when it occurs should be equal to the ratio 4.8096/7.6634 which approximately equals 0.63 (1/1.6). Figure 7(*b*) of the Cruickshank & Munson paper (1981) shows this to be so. The ratio between the two transition points clearly approximates the value indicated above.

8. Conclusions

A theoretical analysis of the problem of fluid buckling has been performed and comparisons with experimental data show quite good agreement, the slight divergence between theory and experiment probably being accounted for by surface tension effects and changes in the jet profiles that were ignored in the models.

Professor Bruce R. Munson's help in the completion of this work through very useful and lengthy discussions, is gratefully acknowledged.

REFERENCES

BASSET, A. B. 1894 Waves and jets in a viscous liquid. *Am. J. Maths.* **16**, 93–110.

BATCHELOR, G. K. & GILL, A. E. 1962 Analysis of the stability of axisymmetric jets. *J. Fluid Mech.* **14**, 529–551.

BEJAN, A. 1987 Buckling flows: a new frontier in fluid mechanics. *Annual Review of Numerical Fluid Mechanics and Heat Transfer* (ed. T. C. Chawla), pp. 262–304. Hemisphere.

BOLOTIN, V. V. 1964 *The Dynamic Stability of Elastic Systems.* San Francisco: Holden-Day.

Cruickshank, J. O. 1980 Viscous fluid buckling: a theoretical and experimental analysis with extensions to general fluid stability. Ph.D. dissertation, Iowa State University, Ames, Iowa.

Cruickshank, J. O. 1987 A new method for predicting the critical Taylor number in rotating cylindrical flows. *J. Appl. Mech.* **54**, 713–719.

Cruickshank, J. O. & Munson, B. R. 1981 Viscous fluid buckling of plane and axisymmetric jets. *J. Fluid Mech.* **113**, 221–239.

Cruickshank, J. O. & Munson, B. R. 1982 An energy loss coefficient in fluid buckling. *Phys. Fluids* **25**, 1935–1937.

Cruickshank, J. O. & Munson, B. R. 1983 A theoretical prediction of the fluid buckling frequency. *Phys. Fluids* **24**, 928–930.

Swope, R. D. & Ames, W. F. 1963 Vibrations of a moving threadline. *J. Franklin Inst.* **275**, (1), 37–55.

Taylor, G. I. 1968 Instability of jets, threads and sheets of viscous fluid. *Proc. Intl. Congr. Appl. Mech.* Springer.